Journal of King Saud University – Computer and Information Sciences xxx (2018) xxx–xxx

Contents lists available at ScienceDirect

Journal of King Saud University – Computer and Information Sciences

journal homepage: www.sciencedirect.com

Comparative analysis of integer wavelet transforms in reversible data hiding using threshold based histogram modification

Ahmad Shaik, V. Thanikaiselvan *

Department of Communication Engineering, School of Electronics Engineering (SENSE), VIT University, Vellore 632014, Tamilnadu, India

ARTICLE INFO

Article history:
Received 8 February 2018
Revised 15 May 2018
Accepted 3 June 2018
Available online xxxx

Keywords:
Integer-to-integer wavelet transforms
Image reversible data hiding
Lifting scheme
Transform domain data hiding
Histogram shifting

ABSTRACT

In the secured data communication scenario, image based Reversible Data Hiding (RDH) at transform domain is receiving its due popularity now. In research works so far, evaluation of transforms in RDH is very minor compared to that of image coding. Since both the areas deal primarily with integers, the present study takes an appreciable step forward by investigating the utilization of integer-to-integer wavelet transforms that have reversibility, which helped in developing high capacity and robust RDH algorithms. The proposed investigation tends to bridge gaps in the area of data hiding with the available coding transforms. In this work, integer wavelet transforms like Haar, 5/3, 2/6, 9/7-M, 2/10, 5/11-C, 5/11-A, 6/14, 13/7-T, 13/7-C and 9/7-F are evaluated using a generalized threshold-based histogram shifting technique. This work compares the performance of all integer wavelet transforms and other state of the art techniques with respect to their embedding capacity and image visual quality. This analysis leads to a better understanding of the relationship between the embedding capacity and the stego image quality whenever different wavelets were utilized.

1. Introduction

Information security is one of the most challenging areas in digital era (Shi et al., 2016; Bibi et al., 2018) . The concept of reversible data hiding (RDH) in images has received increased attention in recent years (Shi et al., 2016; Thanikaiselvan et al., 2017; Shaik et al., 2017; Muhammad et al., 2017). RDH techniques are basically classified into compression, spatial and transform domain RDH techniques. In the process of data hiding, the compression-based techniques create space in the cover image using lossless compression techniques to hide secret data; the spatial techniques directly modify the cover image pixels to hide secret data; and transform domain techniques first, converts the cover image into the frequency domain and then modifies the transformed coefficients to hide secret data.

The spatial and compression domain techniques modify the pixel intensities directly, hence the robustness of these techniques is less (Tsai, 2009; Qin et al., 2013; Lin and Liu, 2012). Whereas in transform domain the transformed image coefficients are altered to store data which improves the robustness. Hence, there has been a growing interest in transforms for image RDH applications (Fridrich et al., Aug. 2001; Muhammad et al., 2015) . But standard transforms like discrete cosine transform (DCT) (Nikolaidis, 2015; Lin, 2012) and discrete wavelet transform (DWT) (Chan et al., 2009; Huang and Chang, 2011; Chang et al., 2010; Li et al., 2017) produce real valued coefficients in the transform domain as shown in Fig. 1. So, the quantization process is mandatory to get the integer coefficients. It increases the complexity of the process. Since all the coefficients in DCT and DWT are real valued, techniques employing these transforms require more auxiliary data to take care of the fractional part which is essential for cover image recovery. This auxiliary data leads to a reduction in the capacity of hiding as well as visual quality. In contrast, the reversible integer-to-integer wavelet transforms convert the spatial domain pixels into transform domain integer coefficients. Hence, these transforms are suitable for data embedding which can offer higher embedding capacity and better visual quality. Thus, reversible

* Corresponding author.
E-mail addresses: shaik.ahmad@vit.ac.in (A. Shaik), thanikaiselvan@vit.ac.in (V. Thanikaiselvan).
URLs: http://livedna.net/?dna=91.15521 (A. Shaik), http://livedna.org/91.13655 (V. Thanikaiselvan).

Peer review under responsibility of King Saud University.

Production and hosting by Elsevier

https://doi.org/10.1016/j.jksuci.2018.06.001
1319-1578/

Please cite this article in press as: Shaik, A., Thanikaiselvan, V. Comparative analysis of integer wavelet transforms in reversible data hiding using threshold based histogram modification. Journal of King Saud University – Computer and Information Sciences (2018), https://doi.org/10.1016/j.jksuci.2018.06.001

229	204	249	249
241	130	250	183
134	155	138	227
243	192	250	136

(a) Input

802.5	-10.88	18.5	74.32
56.22	-35.24	25.49	7.27
73.5	39.85	-37.5	16.5
-34.11	-61.72	19.74	-96.75

(b) DCT

402	465.5	31	32.5
362	375.5	-73	-10.5
68	33.5	-43	-33.5
15	12.5	-36	-101.5

(c) DWT (Haar)

200	232	-68	-34
180	187	-15	-13
-31	-33	-86	-67
73	11	-72	-203

(d) Integer wavelet (Haar)

Fig. 1. DCT, DWT and integer wavelet forward transformation.

integer wavelets can be more suitable for RDH algorithms (Agrawal and Kumar, 2016).

In general, the embedding process in transform domain is carried out using spatial RDH techniques like histogram shifting (Ni et al., 2006) and difference expansion (Tian, 2003). Histogram shifting modifies the cover image histogram to hide secret data. Since the capacity depends on the peak points of the histogram, direct histogram modification offers a very low embedding capacity. As an extension to it, difference based histogram modification (Tai et al., 2009; Liu et al., 2015) and transform domain histogram modification (Wu and Zheng, 2011; Jinna and Ganesan, 2010; Yang et al., 2007; Arsalan et al., 2012; Muhammad, 2017) techniques are implemented. In transform domain, the integer wavelet classifies the cover image data and produces the histogram with high peaks which support high embedding capacity.

There is a growing body of literature that recognizes the importance of histogram shifting in integer wavelet based RDH technique (Shi et al., 2016). Hence in our work, we have selected a generalized threshold based histogram shifting (Lee et al., 2006) as a common embedding technique to evaluate the performance of the integer wavelet transforms.

From the literature, it has been observed that the research on wavelets is focussed more towards compressive applications (Calderbank et al., 1998; Le Gall and Tabatabai, 1988; Villasenor et al., 1995; Strang and Nguyen, 1996; Gormish et al., 1997; Adams and Kossentini, 1999; Adams and Kossentini, 2000). Since both areas deal primarily with integers, the present study is intended further investigate the use of reversible integer wavelets for the development of high capacity and robust RDH algorithms. The proposed investigation helps to fill the gap in the area of data hiding with the available coding transforms. In this paper, we report the results of that study, with the following contributions:

We give a brief description of image transformation using wavelet transforms and mentioned the mathematical representation of popular integer wavelet transforms like Haar, 5/3, 2/6, 9/7-M, 2/10, 5/11-C, 5/11-A, 6/14, 13/7-T, 13/7-C and 9/7-F (Section 2).

The operation of threshold-based histogram shifting in the transform domain is explained with steps and block diagram in Section 3. We explain the flag array-based overflow/underflow compensation technique in Section 3.2.

The performances of all the transforms are evaluated concerning Peak Signal to Noise Ratio (PSNR), Structural Similarity Index (SSIM) and bit rate as bits per pixel (bpp). Along with that, all the transforms are compared with state of the art spatial domain, DCT, DWT and integer wavelet transforms based standard RDH algorithms (Section 4).

In this paper, several integer wavelet transforms are compared by their performance in threshold-based histogram shifting technique.

2. Integer-to-Integer Wavelet Transforms

These transforms are derived from the linear wavelet functions which support invertibility. Unlike the standard DWT, the integer versions are invertible in finite precision arithmetic with less computational complexity. Hence, these transforms are very useful in data hiding applications, where the cover medium requires integers (Muhammad et al., 2017; Muhammad and Bibi, 2015) .

The integer wavelet transforms used in this paper are taken from the Sweldens' lifting scheme (Sweldens, 1995) and wavelet construction technique (Calderbank et al., 1998). Arithmetic operations of Fixed Point type are used in the transform implementation. Specifically, these operations are integer addition, multiplication, subtraction as well as division. Here the approximation of all the transforms' filter coefficients is carried out using rational numbers of dyadic type; hence multiplication and division operations can be calculated by using simple bit shifts. Two's complement is used to represent the negative numbers. The 1D representation of the forward integer wavelet transforms given in Table 1. A sign change in approximation and detail formulae provide the inverse integer type wavelet transforms, hence those are not added.

The signal notations described in this paper should be followed for a better understanding of forward transform equations. All these transforms used in this work uses linear-phase finite impulse response (FIR) filters with a filter bank structure containing a bank of filters. A filter bank is a combination of analysis and synthesis parts, and each part is a combination of approximation and detail sub-band filters. Here $x[n]$, $a[n]$ and $d[n]$ are used to represent input signal, approximate (lowpass filter) coefficients and detail (high pass filter) coefficients respectively. These transforms are named with x/y notation to mention that the basic filter bank has x low pass, and y high pass analysis filters coefficients. Further, the even $x[n]$ signal is represented as $a_0[n]$=$x[2n]$ and the odd $x[n]$ signal is represented as $d_0[n]$=x[$2n$ + 1]. Symmetric extension strategy is used in the boundaries of the finite length signals. The Table 1, represents the floor function.

In image decomposition, first, an image of size $M \times N$ is applied to a wavelet transform by considering each row of length N as a 1D signal. After forward transform the input 1D signal split into two parts each of size $\frac{N}{2}$. This operation is called a row processing. It repeats for M rows and produces two sub-band signals viz., the low frequency band (L) and high frequency band (H) of size $M \times \frac{N}{2}$. Then L and H parts are independently applied to wavelet transform by considering each column of size M as a 1D signal. This operation is known as column processing. It divides each band (L and H) into two sub-bands of size $\frac{M}{2} \times \frac{N}{2}$. Where L band produces an approximation (LL) and vertical (LH) sub-bands; H band produces horizontal (HL) and diagonal (HH) sub-bands. In the transformed cover image, the approximation component (LL) holds

Please cite this article in press as: Shaik, A., Thanikaiselvan, V. Comparative analysis of integer wavelet transforms in reversible data hiding using threshold based histogram modification. Journal of King Saud University – Computer and Information Sciences (2018), https://doi.org/10.1016/j.jksuci.2018.06.001

Table 1
Forward Transforms.

Haar	$d[n] = d_0[n] - a_0[n]$ $a[n] = a_0[n] + \lfloor \frac{1}{2} d[n] \rfloor$
5/3; (Calderbank et al., 1998); (Le Gall and Tabatabai, 1988)	$d[n] = d_0[n] - \lfloor \frac{1}{2}(a_0[n+1] + a_0[n]) \rfloor$ $a[n] = a_0[n] + \lfloor \frac{1}{4}(d[n] + d[n-1]) + \frac{1}{2} \rfloor$
2/6; (Villasenor et al., 1995)	$d_1[n] = d_0[n] - a_0[n]$ $a[n] = a_0[n] + \lfloor \frac{1}{2} d_1[n] \rfloor$ $d[n] = d_1[n] + \lfloor \frac{1}{4}(-a[n+1] + a[n-1]) + \frac{1}{2} \rfloor$
9/7-M; (Calderbank et al., 1998);	$d[n] = d_0[n] + \lfloor \frac{1}{16}((a_0[n+2] + a_0[n-1]) - 9(a_0[n+1] + a_0[n])) + \frac{1}{2} \rfloor$ $a[n] = a_0[n] + \lfloor \frac{1}{4}(d[n] + d[n-1]) + \frac{1}{2} \rfloor$
2/10; (Gormish et al., 1997)	$d_1[n] = d_0[n] - a_0[n]$ $a[n] = a_0[n] + \lfloor \frac{1}{2} d_1[n] \rfloor$ $d[n] = d_1[n] + \lfloor \frac{1}{64}(22(a[n-1] - a[n+1]) + 3(a[n+2] - 2a[n-2])) + \frac{1}{2} \rfloor$
5/11-C; (Calderbank et al., 1998)	$d_1[n] = d_0[n] - \lfloor \frac{1}{2}(a_0[n+1] + a_0[n]) \rfloor$ $a[n] = a_0[n] + \lfloor \frac{1}{4}(d_1[n] + d_1[n-1]) + \frac{1}{2} \rfloor$ $d[n] = d_1[n] + \lfloor \frac{1}{16}(a[n+2] - a[n+1] - a[n] + a[n-1]) + \frac{1}{2} \rfloor$
5/11-A; (Adams and Kossentini, 1999)	$d_1[n] = d_0[n] - \lfloor \frac{1}{2}(a_0[n+1] + a_0[n]) \rfloor$ $a[n] = a_0[n] + \lfloor \frac{1}{4}(d_1[n] + d_1[n-1]) + \frac{1}{2} \rfloor$ $d[n] = d_1[n] + \lfloor \frac{1}{32}(a[n+2] - a[n+1] - a[n] + a[n-1]) + \frac{1}{2} \rfloor$
6/14; (Adams and Kossentini, 2000)	$d_1[n] = d_0[n] - a_0[n]$ $a[n] = a_0[n] + \lfloor \frac{1}{16}(-d_1[n+1] + d_1[n-1] + 8d_1[n]) + \frac{1}{2} \rfloor$ $d[n] = d_1[n] + \lfloor \frac{1}{16}(a[n+2] - a[n-2] + 6(-a[n+1] - 2a[n-1])) + \frac{1}{2} \rfloor$
13/7-T; (Calderbank et al., 1998)	$d[n] = d_0[n] + \lfloor \frac{1}{16}((a_0[n+2] + a_0[n-1]) - 9(a_0[n+1] + a_0[n])) + \frac{1}{2} \rfloor$ $a[n] = a_0[n] + \lfloor \frac{1}{32}((-d[n+1] - d[n-2]) + 9(d[n] + d[n-1])) + \frac{1}{2} \rfloor$
13/7-C; (Adams and Kossentini, 2000)	$d[n] = d_0[n] + \lfloor \frac{1}{16}((a_0[n+2] + a_0[n-1]) - 9(a_0[n+1] + a_0[n])) + \frac{1}{2} \rfloor$ $a[n] = a_0[n] + \lfloor \frac{1}{16}(5(d[n] + d[n-1]) - (d[n+1] + d[n-2])) + \frac{1}{2} \rfloor$
9/7-F; (Calderbank et al., 1998)	$d_1[n] = d_0[n] - \lfloor \frac{1}{128}(203(-a_0[n+1] - a_0[n])) + \frac{1}{2} \rfloor$ $a_1[n] = a_0[n] + \lfloor \frac{1}{4096}(217(-d_1[n] - d_1[n-1])) + \frac{1}{2} \rfloor$ $d[n] = d_1[n] - \lfloor \frac{1}{128}(113(a_1[n+1] + a_1[n])) + \frac{1}{2} \rfloor$ $a[n] = a_1[n] + \lfloor \frac{1}{4096}(1817(d_1[n] + d_1[n-1])) + \frac{1}{2} \rfloor$

the most significant features and looks identical to the cover image. This successive row and column transformations are treated as one-level wavelet decomposition. The second-level decomposition can be performed by considering the approximation sub-band as the input image.

Although the orders of operations for the forward transformation can be changed, the inverse transformation must perform the same operations as that of forward transform but in the reverse order; otherwise, perfect reversibility cannot be guaranteed.

3. Data hiding using integer wavelet transforms

This section explains the operation of threshold-based histogram shifting in the transform domain. In the process of data hiding, a one level decomposition is applied to the cover image I using a selected integer wavelet transform. The decomposed cover image is noted as I_{Dec}. Then the data hiding is performed on the detail sub-bands (*LH*, *HL*, and *HH*) coefficients. After that, the intermediate stego image is obtained by doing the inverse transformation using the same integer wavelet transform. Then overflow compensation technique is performed to obtain final stego image I' by eliminating the overflow and underflow pixels. The process of data hiding in the transform domain is shown in Fig. 2, where the shaded portion of components represents the alteration using the histogram shifting.

The order of the extraction process closely resembles the embedding process. At the receiver end, the stego image overflow and under flow pixels are converted back to their original values using the flag array. Then we decompose the image using the same integer wavelet transform which is used at the embedding stage. After that, the threshold-based histogram shifting extracts the secret data from detail sub-bands (*LH′*, *HL′*, and *HH′*) and restores the original sub-bands (*LH*, *HL*, and *HH*). Finally, obtains the original cover image I by performing the inverse transformation on original approximation (*LL*) and restored detail sub-bands.

3.1. Proposed threshold based histogram shifting

In modern RDH techniques, the difference histogram modification is considered as one of the prominent building blocks for data hiding. In this paper, a modified threshold-based histogram shifting method is proposed for data hiding. It is quite suitable for both spatial and transform techniques and offers high embedding capacity with a limited distortion (Lee et al., 2006).

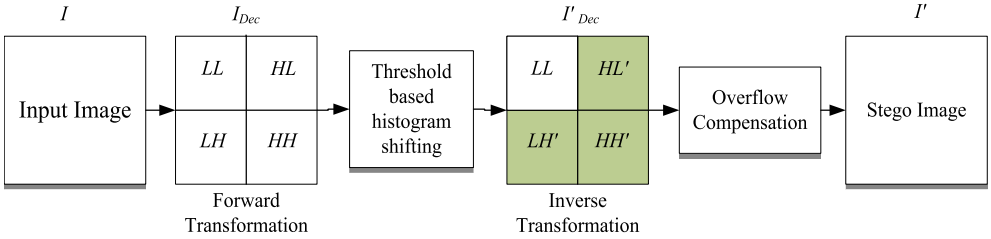

Fig. 2. Threshold based histogram shifting in transform domain.

Please cite this article in press as: Shaik, A., Thanikaiselvan, V. Comparative analysis of integer wavelet transforms in reversible data hiding using threshold based histogram modification. Journal of King Saud University – Computer and Information Sciences (2018), https://doi.org/10.1016/j.jksuci.2018.06.001

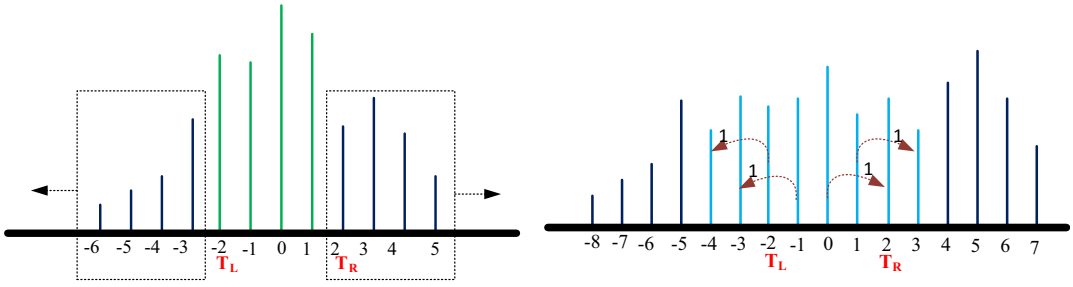

(a) Input histogram (b) Histogram after data hiding

Fig. 3. Threshold based histogram shifting.

Let us consider an integer wavelet transformed cover image I of size $M \times N$ ranges from $-\infty$ to ∞ and the thresholds $[T_L, T_R)$. The embedding capacity of I is equal to the total bin count which falls in the range $T_L \leq I < T_R$. Here, the image pixels are selected one at a time in a raster scan order. For a selected pixel $I(i, j) = p$, the data hiding is performed using Eq. (1), where i and j represent the row and column index of that pixel respectively. Depends on the secret data size, here we can adjust the threshold parameters. To hide a larger secret data, we can select a higher threshold value.

$$p' = \begin{cases} p + T_L & if \quad p < T_L \quad or \quad (T_L \leqslant p < 0 \& d = 1) \\ p + T_R & if \quad p \geqslant T_R \quad or \quad (0 \leqslant p < T_R \& d = 1) \\ p & if \quad (T_L \leqslant p < 0 \& d = 0) \quad or \quad (0 \leqslant p < T_R \& d = 0) \end{cases} \tag{1}$$

Here p' is the altered coefficient value from stego image location $I'(i, j)$ and $d \in \{0,1\}$ is the secret bit value. In histogram modification, the bins lesser than T_L are shifted to the left by $|T_L|$ positions and similarly the bins equal or higher than T_R are shifted to the right by T_R positions. This shifting results in the empty bins in the ranges $[2T_L\ T_L)$ and $[T_R, 2T_R)$. The bins under the range $[T_L, T_R)$ are changed according to the secret data, for a selected coefficient if the secret bit is 0 then no change occurs in that coefficient; if the secret bit is one then shifting happens. The pictorial representation of threshold-based histogram shifting for thresholds $[-2, 2)$ is shown in Fig. 3.

While extracting the data, the image is scanned in the same raster scan manner. If the scanned value falls in the range $[2T_L, T_L)$ or $[T_R, 2T_R)$, it indicates that the secret bit embedded is 1. If the scanned value falls in the range $[T_L, T_R)$, it indicates that the secret bit embedded is 0. After extracting the embedded data, the original image coefficients can be restored using Eq. (2).

$$p = \begin{cases} p' - T_L & if \quad p' < T_L \\ p' - T_R & if \quad p' \geqslant T_R \\ p' & if \quad T_L \leqslant p' < T_R \end{cases} \tag{2}$$

Since, the histogram consists of integer transformed image coefficients which are natural integers ranging from $(-\infty, +\infty)$, the overflow and underflow problems may occur. Therefore, here a "flag array" method (Ma and Shi, 2016) is used to record the underflow/overflow pixels. In flag array method, the underflow/overflow pixels would be prevented by shrinking the histogram in both sides.

3.2. Flag array method for overflow compensation

RDH systems after hiding the secret data in the integer wavelet coefficients, inverse transformation will be performed to achieve the spatial stego image. During this process, overflow/underflow pixels may occur. That is for an eight-bit grayscale image, the values of some pixels in the stego image may be beneath the lower bound 0 and/or will exceed the upper bound 255. Here a "flag array" method (Ma and Shi, 2016) is used to record the underflow/overflow pixels by shrinking the histogram of the intermediate stego image.

3.3. Data embedding process

The data hiding consists of the following steps:

Step 1: Take an input image I of size $M \times N$ along with secret data D and thresholds $[T_L, T_R)$.

Step 2: Apply the one-level integer wavelet transformation on the cover image I and obtain one approximation (LL), and three detail sub-bands (HL, LH, and HH) each of size $\frac{M}{2} \times \frac{N}{2}$.

Step 3: Combine the three-high frequency sub-bands, HL, LH, and HH, to make a new coefficient image of size $\frac{3M}{4} \times N$.

Step 4: Hide the secret data D on the detail sub-bands of the cover image using threshold-based histogram shifting on the new coefficient image accord.

Step 5: After data hiding split the modified image of size $\frac{3M}{4} \times N$ into three equal sub-bands viz., HL', LH', and HH' each of size $\frac{M}{2} \times \frac{N}{2}$.

Step 6: Obtain the intermediate stego image of size $M \times N$ by performing the 1D inverse integer wavelet transform (same transform used in step 2) on the original approximation sub-band (LL) and the modified detail sub-bands (HL', LH', and HH').

Step 7: Finally, perform the overflow compensation mechanism and obtain the final stego image I' and its respective flag array.

The parameters such as thresholds, flag array details should be communicated to the receiver for a loss less data extraction. Here we will embed the threshold values and the flag array data into the first row and first column of the cover image using LSB substitution (Zhang and Ping, Oct. 2003). The original LSB positions of that pixels are embedded into the cover image along with the secret message.

Fig. 4, presents the overall process of threshold-based histogram shifting based on integer wavelet transform. Here we have considered the image Lena as a cover, integer Haar wavelet as transform and $[-2,2)$ as predefined thresholds. It shows the output of each step along with the respective histogram. It can be seen from Fig. 4(a) and (d) that the cover image histogram and the stego image histogram shapes are highly correlated. Which implies the quality of the stego image is maintained even after the data embedding. The same process can be applied to any cover image using any integer wavelet transform.

3.4. Data extraction process

In the extraction phase we perform the steps identical to the data embedding process but in a reverse order to obtain the secret data as well as the original image without any loss. At the extraction phase initially, we read the LSB positions of the first row and column for threshold details $[T_L, T_R)$ and the flag array information.

Please cite this article in press as: Shaik, A., Thanikaiselvan, V. Comparative analysis of integer wavelet transforms in reversible data hiding using threshold based histogram modification. Journal of King Saud University – Computer and Information Sciences (2018), https://doi.org/10.1016/j.jksuci.2018.06.001

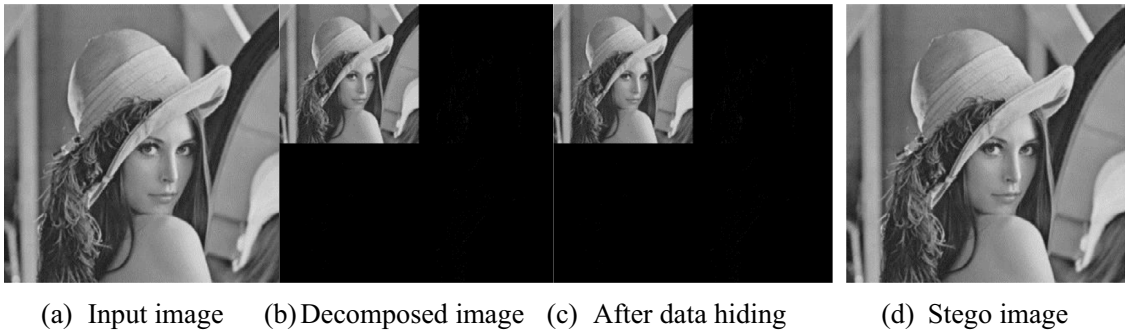

(a) Input image (b) Decomposed image (c) After data hiding (d) Stego image

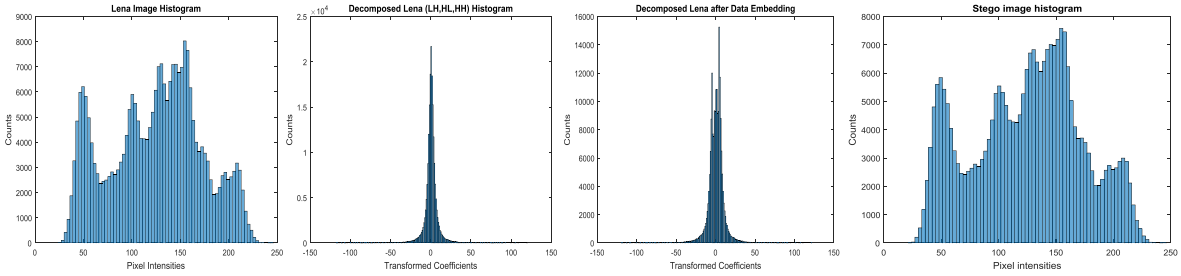

(a) Input histogram (b) LH, HL, HH histogram (c) After data embedding (d) Stego image histogram

Fig. 4. Overall process using Lena Image.

After extracting these details, we perform the data extraction operation. The steps involved in the data extraction process are described as follows:

Step 1: Consider the stego image I' of size $M \times N$ and perform the inverse flag array operation by expanding the stego image histogram to its original range.

Step 2: Apply the one-level integer wavelet transformation on the cover image and obtain one approximation (LL), and three modified detail sub-bands (HL', LH', and HH') each of size $\frac{M}{2} \times \frac{N}{2}$.

Step 3: Combine the three-modified high frequency sub-bands to make a new coefficient image of size $\frac{3M}{4} \times N$

Step 4: Extract the secret data D from the new coefficient image using threshold-based histogram shifting and restore the original detail sub-band coefficient image.

Step 5: After data extraction separate the restored coefficient image into three equal sub-bands viz., HL, LH, and HH each of size $\frac{M}{2} \times \frac{N}{2}$.

Step 6: Restore the cover image I by performing the inverse integer wavelet transformation on the original approximation sub-band (LL) and the restored detail sub-bands (HL, LH, and HH).

4. Results and discussion

In this paper, eleven images from the USC-SIPI database of size 512×512 are considered for the experiment which includes Airplane, Baboon, Elaine, Tree, Boat, House, Home, Lady, Lena, Peppers, and Tanker as shown in Fig. 5. On these eleven images, histogram shifting is performed using integer wavelets with 30 different threshold values like from $[-1\ 1)$ to $[-30\ 30)$. PSNR (Eq. (3)), SSIM (Eq. (4)), and bit rate (Eq. (5)) are considered as evaluation parameters.

$$PSNR(dB) = 10\log_{10}\left(\frac{255 \times 255}{\frac{1}{MN}\sum_{p=1}^{M}\sum_{q=1}^{N}(I(i,j) - I'(i,j))^2}\right) \quad (3)$$

Here I and I' are the cover image and stego image of size $M \times N$ respectively.

$$SSIM = \frac{(2\mu_I\mu_{I'} + k_1)(2\sigma_{I,I'} + k_2)}{(\mu_I^2 + \mu_{I'}^2 + k_1)(\sigma_I^2 + \sigma_{I'}^2 + k_2)} \quad (4)$$

where μ_I, ${\sigma_I}^2$, $\mu_{I'}$ and ${\sigma_{I'}}^2$ are mean and variances of the cover image and stego image respectively. $\sigma_{I,I'}$ is the covariance between both images; k_1, k_2 are two constants used to avoid divide by zero situations. The SSIM value ranges between [0, 1], where 0 refers to the least similarity while close to 1 refers to the highest.

$$Bitrate(bpp) = \frac{Secretdatasize(bits)}{Totalnumberofpixels} \quad (5)$$

In general, the spatial domain RDH techniques uses very simple arithmetic operations to directly manipulate the cover image pixels. Where as in the transform domain RDH techniques the data hiding is performed on the frequency coefficients of the cover image. The transform domain techniques need one additional operation as compared to the spatial domain technique hence, they are more complex as compared to the spatial domain techniques.

Among the proposed integer wavelet transforms, the transforms which have the high scaling factors are complex as compared to the transforms which have low scaling factors. The computations required for performing a one-level wavelet decomposition for a one-dimensional signal are given in Table 2 (Adams and Kossentini, 2000). The numbers in the brackets indicate computations for hardware or software implementations where multiplications are costlier than addition and shift operations. Though most of the transforms involve the same number of calculations, some need more multiplications than others. In particular, the underlying lifting filters for Haar, 5/3, 2/6, 5/11-C and 5/11-A transforms have coefficients that are powers of two. Evidently, haar transform requires least computation followed by the 5/3 and 2/6 group, followed by the 9/7-M, 2/10, 5/11-C and 5/11-A group and then the 6/14, 13/7-T, and 13/7-C group. Lastly the 9/7-F transform requires the more computations.

Please cite this article in press as: Shaik, A., Thanikaiselvan, V. Comparative analysis of integer wavelet transforms in reversible data hiding using threshold based histogram modification. Journal of King Saud University – Computer and Information Sciences (2018), https://doi.org/10.1016/j.jksuci.2018.06.001

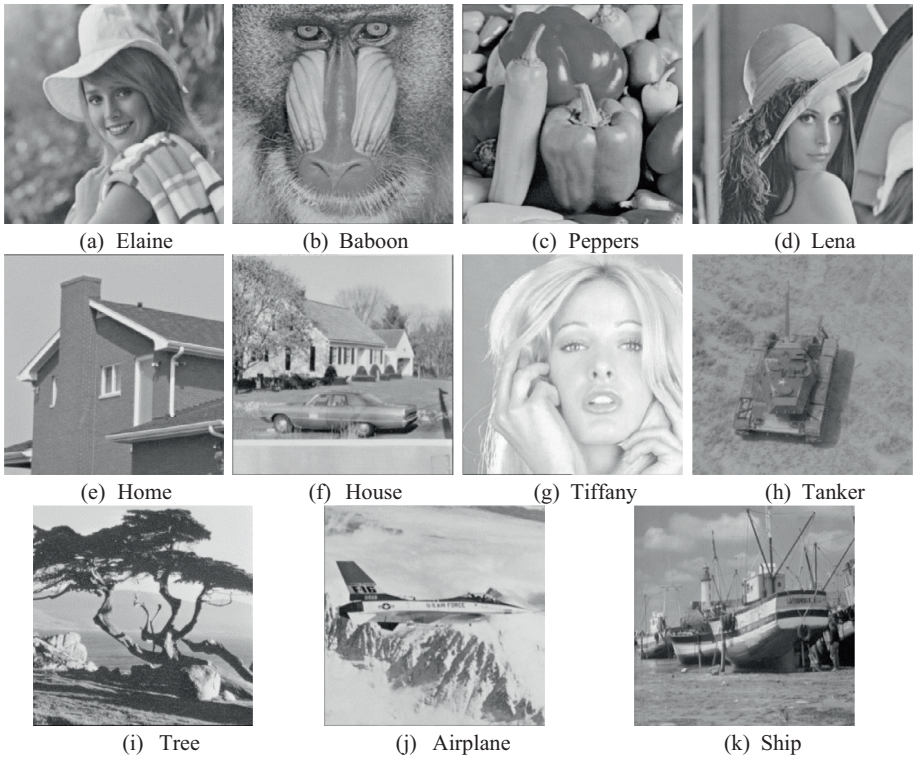

Fig. 5. Input Images.

Table 2
Computation complexity.

Transform	Additions	Shifts	Multiplies	Total
Haar	2	1	0	3
5/3	5	2	0	7
2/6	5	2	0	7
9/7-M	8 (9)	2 (3)	1 (0)	11 (12)
2/10	7 (10)	2 (6)	2 (0)	11 (16)
5/11-C	10	3	0	13
5/11-A	10	3	0	13
6/14	10 (11)	3 (5)	1 (0)	14 (16)
13/7-T	10 (12)	2 (4)	2 (0)	14 (16)
13/7-C	10 (12)	2 (4)	2 (0)	14 (16)
9/7-F	12 (26)	4 (18)	4 (0)	20 (44)

Table 3 represents the PSNR and embedding capacities (bit rate) of the stego images when the threshold values are [−1 1). Similarly, with thresholds ranging from [−1,1) to [−30, 30), same process is carried out and their average responses are represented in Table 4. In Table 3, the last rows represent the average PSNR and bit rate of each transform. From the results, it is noted that, the low-valued transforms like Haar, 5/3, 2/6 and 2/10 are providing a little higher PSNR compared to 5/11-C, 5/11-A, and 6/14. But these transforms are obtaining slightly less bit-rate as compared with the same transforms. Overall integer Haar wavelet is providing the highest PSNR with lowest embedding capacity because its lower valued scaling factors. While 3/7-T and 9/7-F transforms are giving a poor PSNR value for all images because of their larger scaling factors.

Fig. 6, presents the performance of the integer wavelet transforms with respect to bit rate and PSNR for 30 different threshold values starting from [−1, 1) to [−30, 30). Here we have shown the results of six cover images including Elaine, Baboon, Lena and Airplane, Peppers and Tree. From the Fig. 6, it can be noted that the smaller thresholds have smaller embedding capacity and high visual quality. Since the changes made in the cover image is small the visual quality at the smaller thresholds are high. As the threshold values are high, more cover image coefficients are used for data hiding which leads to more distortion. We have observed that as the threshold values are increasing further and further, the change in the embedding capacity and the visual quality are decreased. At one particular point the effect of thresholds on the embedding capacity and PSNR reached almost negligible.

For example, in Fig. 6(a) the PSNR and bit rate of Haar transform at thresholds [−1, 1) are 48.31 dB and 0.1 bpp respectively. As the thresholds increased one position the PSNR valued decreased nearly 3.4 dB and the bit rate increased nearly 0.085 bpp. If perform the same operation between the threshold values [−15, 15) and [−16, 16), the PSNR change decreased by 0.18 dB and bitrate increased by 0.01 bpp. From the experiment, the threshold values greater than [−15, 15) has minimum effect on embedding capacity and PSNR. Over all for lower threshold values the transforms like Haar, 2/6 and 2/10 performed well as compared to the larger scaling factor transforms. Similarly for high threshold values, the larger scaling factor wavelets like 13/7-C, 6/14, 9/7-M, 5/11-C, and 9/7-F achieved a good trade-off between bit-rate and PSNR. On the whole, 2/10 and 2/6 gave relatively better bit rate as well as PSNR for all thresholds.

The performance of wavelet transforms concerning SSIM and bit rate are shown in Fig. 7. Similar to Fig. 6, here also we calculated SSIM values for 30 different thresholds. Transforms like Haar, 2/6 and 2/10 maintaining relatively a constant and a high SSIM followed by 13/7-C, 6/14, 9/7-F and 5/11-C transforms. From the Fig. 7, it is clear that 13/7-T provides a relatively low SSIM value because of its high scaling factor values.

The performance of the wavelets compared with other state of the art techniques is shown in Table 5. For this evaluation, the images Lena, Baboon, Plane, and Boat are considered. The last column represents the average PSNR and bit rate of existing method and transform. From Table 5 Airplane image it is noted that the

Please cite this article in press as: Shaik, A., Thanikaiselvan, V. Comparative analysis of integer wavelet transforms in reversible data hiding using threshold based histogram modification. Journal of King Saud University – Computer and Information Sciences (2018), https://doi.org/10.1016/j.jksuci.2018.06.001

Table 3
PSNR and bit rate for thresholds [−1 1).

Image	Metric	Haar	5/3	2/6	9/7-M	2/10	5/11-C	5/11-A	6/14	13/7-T	13/7-C	9/7-F
Elaine	PSNR	48.31	48.28	48.17	48.07	48.12	48.12	48.20	48.04	47.69	47.96	45.29
	Bit rate (bpp)	0.100	0.112	0.105	0.112	0.104	0.110	0.112	0.109	0.094	0.115	0.118
Baboon	PSNR	48.21	48.14	48.03	47.93	47.98	47.95	48.04	47.96	47.38	47.84	45.46
	Bit rate (bpp)	0.050	0.064	0.056	0.067	0.057	0.065	0.066	0.059	0.059	0.065	0.067
Fruits	PSNR	48.36	48.27	48.22	48.05	48.17	48.10	48.22	48.08	47.70	47.98	45.21
	Bit rate (bpp)	0.124	0.137	0.134	0.139	0.134	0.136	0.137	0.138	0.104	0.142	0.146
Home	PSNR	48.50	48.05	48.29	47.87	48.23	47.92	47.98	48.14	47.29	47.83	45.37
	Bit rate (bpp)	0.206	0.224	0.219	0.234	0.220	0.223	0.225	0.218	0.223	0.236	0.238
House	PSNR	48.48	48.03	48.34	47.84	48.26	47.89	47.97	48.14	47.31	47.80	45.30
	Bit rate (bpp)	0.202	0.224	0.223	0.240	0.227	0.227	0.228	0.221	0.229	0.241	0.236
Tiffany	PSNR	48.45	48.25	48.29	48.03	48.27	48.08	48.19	48.16	47.50	47.91	45.25
	Bit rate (bpp)	0.174	0.195	0.187	0.201	0.189	0.195	0.196	0.189	0.186	0.203	0.205
Lena	PSNR	48.39	48.23	48.25	48.02	48.20	48.04	48.17	48.13	47.50	47.94	45.25
	Bit rate (bpp)	0.153	0.184	0.171	0.188	0.173	0.184	0.185	0.176	0.174	0.188	0.191
Plane	PSNR	48.53	48.10	48.36	47.89	48.30	47.96	48.06	48.20	47.43	47.84	45.35
	Bit rate (bpp)	0.218	0.239	0.235	0.258	0.238	0.243	0.243	0.234	0.246	0.259	0.258
Boat	PSNR	48.33	48.23	48.22	48.01	48.18	48.08	48.16	48.09	47.55	47.94	45.26
	Bit rate (bpp)	0.106	0.126	0.119	0.131	0.121	0.130	0.129	0.126	0.107	0.134	0.137
Tanker	PSNR	48.31	48.16	48.15	47.95	48.09	47.97	48.06	48.01	47.41	47.86	45.36
	Bit rate (bpp)	0.099	0.119	0.109	0.120	0.109	0.119	0.120	0.110	0.111	0.120	0.125
Tree	PSNR	48.45	48.10	48.21	47.87	48.17	47.98	48.08	48.09	47.41	47.84	45.41
	Bit rate (bpp)	0.156	0.158	0.157	0.163	0.156	0.155	0.159	0.150	0.150	0.164	0.165
Average	PSNR	48.39	48.17	48.23	47.96	48.18	48.01	48.10	48.09	47.47	47.89	45.32
	Bit rate (bpp)	0.144	0.162	0.156	0.168	0.157	0.162	0.164	0.157	0.153	0.170	0.171

Table 4
Average PSNR and bit rate for all thresholds.

Image	Metric	Haar	5/3	2/6	9/7-M	2/10	5/11-C	5/11-A	6/14	13/7-T	13/7-C	9/7-F
Elaine	PSNR (dB)	35.14	35.22	35.74	35.46	35.76	35.28	35.28	35.81	34.36	35.54	35.14
	Bit rate (bpp)	0.578	0.621	0.590	0.610	0.586	0.616	0.620	0.602	0.579	0.618	0.578
Baboon	PSNR (dB)	32.8	32.32	33.00	32.47	33.01	32.37	32.35	33.10	31.75	32.61	32.80
	Bit rate (bpp)	0.390	0.462	0.422	0.463	0.423	0.468	0.467	0.434	0.444	0.464	0.390
Fruits	PSNR (dB)	36.36	36.58	37.10	36.71	37.13	36.55	36.61	37.08	35.38	36.82	36.36
	Bit rate (bpp)	0.631	0.674	0.647	0.669	0.646	0.674	0.676	0.655	0.650	0.669	0.631
Home	PSNR (dB)	36.84	36.45	37.05	36.46	37.00	36.35	36.46	36.99	35.58	36.63	36.84
	Bit rate (bpp)	0.669	0.702	0.686	0.704	0.686	0.705	0.705	0.688	0.702	0.704	0.669
House	PSNR (dB)	35.51	35.24	36.12	35.49	36.22	35.4	35.34	36.3	34.99	35.68	35.51
	Bit rate (bpp)	0.603	0.666	0.642	0.672	0.646	0.674	0.671	0.650	0.669	0.672	0.603
Tiffany	PSNR (dB)	37.15	37.26	37.74	37.43	37.72	37.29	37.26	37.85	36.38	37.55	37.15
	Bit rate (bpp)	0.670	0.700	0.686	0.701	0.685	0.702	0.701	0.689	0.695	0.701	0.670
Lena	PSNR (dB)	36.58	37.15	37.72	37.45	37.89	37.34	37.27	37.97	36.72	37.61	36.58
	Bit rate (bpp)	0.657	0.710	0.692	0.714	0.696	0.716	0.714	0.700	0.711	0.714	0.657
Plane	PSNR (dB)	37.13	37.13	37.88	37.45	38.02	37.33	37.28	38.04	36.91	37.62	37.13
	Bit rate (bpp)	0.662	0.707	0.692	0.714	0.697	0.714	0.712	0.698	0.712	0.714	0.662
Boat	PSNR (dB)	35.08	35.09	35.73	35.35	35.86	35.26	35.19	35.90	34.39	35.50	35.08
	Bit rate (bpp)	0.585	0.649	0.617	0.649	0.618	0.654	0.653	0.627	0.635	0.649	0.585
Tanker	PSNR (dB)	35.26	35.14	35.63	35.27	35.65	35.17	35.15	35.69	34.37	35.41	35.26
	Bit rate (bpp)	0.614	0.672	0.638	0.670	0.639	0.673	0.673	0.646	0.659	0.670	0.614
Tree	PSNR (dB)	34.48	33.87	34.62	34.02	34.61	33.91	33.95	34.62	33.29	34.12	34.48
	Bit rate (bpp)	0.524	0.583	0.550	0.586	0.548	0.590	0.589	0.552	0.574	0.586	0.524
Average	PSNR (dB)	35.67	35.59	36.21	35.78	36.26	35.66	35.65	36.3	34.92	35.92	35.67
	Bit rate(bpp)	0.598	0.650	0.624	0.65	0.625	0.653	0.653	0.631	0.639	0.651	0.598

average embedding rate of all integer transforms and the PSNR are nearly 44% and 3 dB higher than the Haar DWT based RDH technique (Chan et al., 2009). Also, it achieves nearly 3 dB higher PSNR with a similar embedding rate compared to the integer wavelet transform based histogram shifting method (Wu and Zheng, 2011). Similar results can be observed with other wavelet based RDH systems (Jinna and Ganesan, 2010; Yang et al., 2007).

A comparison between the proposed 9/7 integer wavelet and the DWT based RDH method (Huang and Chang, 2011) is shown in Table 6. From the Table 6, it is observed that the integer wavelet transforms provide very good PSNR with relatively same embedding capacities compared to standard wavelets. Between the two proposed 9/7 integer wavelets, 9/7-M provides better PSNR but slightly lower embedding capacities compared to 9/7-F because of its smaller scaling factors.

The evaluation of the proposed system with respect to SSIM is shown in Table 7. For comparison, four standard images of Lena, Baboon, Airplane, and Boat are selected. DCT based RDH systems (Nikolaidis, 2015; Lin, 2012) , integer wavelet transform and genetic algorithm based techniques (Arsalan et al., 2012) are considered for comparison. Here the last row represents the average bit rate, PSNR and SSIM values of each image with all integer wavelet transforms. Compared to (Nikolaidis, 2015), the average embedding rate is nearly four times higher with a 5.14 dB increase in PSNR and 0.1049 increase in SSIM. Compared to (Arsalan et al., 2012), the proposed method provides nearly double the embedding rate with a better PSNR and slightly higher SSIM for Lena image.

Table 8 presents the difference between the histogram distributions of cover image and the stego image. The shown

Please cite this article in press as: Shaik, A., Thanikaiselvan, V. Comparative analysis of integer wavelet transforms in reversible data hiding using threshold based histogram modification. Journal of King Saud University – Computer and Information Sciences (2018), https://doi.org/10.1016/j.jksuci.2018.06.001

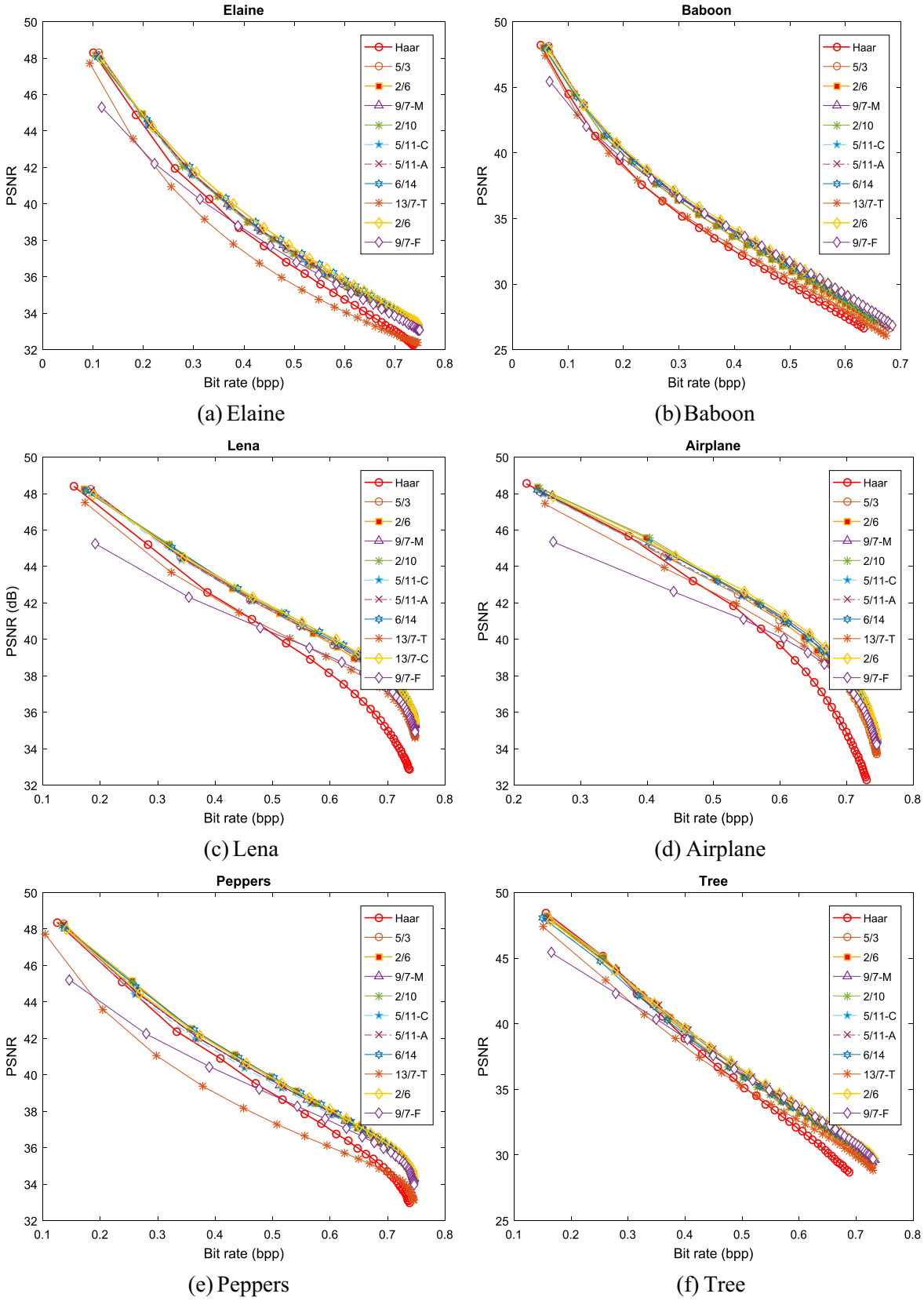

Fig. 6. Performance evaluation concerning bit rate and PSNR.

values are taken from the average of 30 different threshold values. Here we calculated the pairwise Euclidean distance between the pixel intensity and its bin count between the cover image and stego image histograms. It measured the deviation of the stego image histogram from the cover image histogram. The smaller difference suggests the smaller deviation

Please cite this article in press as: Shaik, A., Thanikaiselvan, V. Comparative analysis of integer wavelet transforms in reversible data hiding using threshold based histogram modification. Journal of King Saud University – Computer and Information Sciences (2018), https://doi.org/10.1016/j.jksuci.2018.06.001

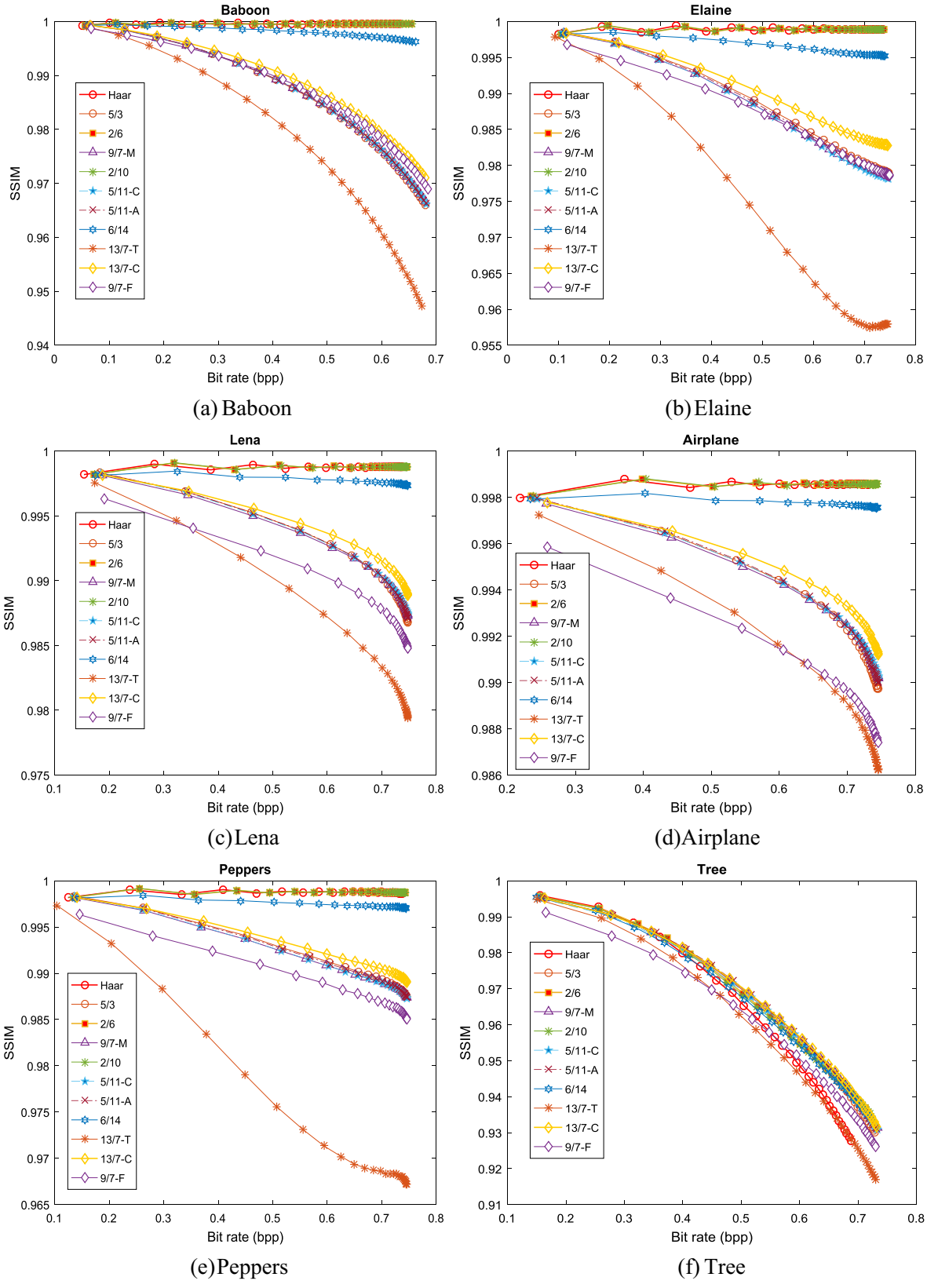

Fig. 7. Performance evaluation concerning bit rate and SSIM.

in the stego image histogram and the larger deviation represents the larger change. From Table 8 it can be noted that, the average values of all transforms are almost identical to each other. Specifically, the Tanker image has recorded highest deviation in the histogram distribution. Without considering the Tanker image the average deviation of all transforms is near to 0.0137, which is almost ten times lesser than the Tanker image histogram deviation.

Please cite this article in press as: Shaik, A., Thanikaiselvan, V. Comparative analysis of integer wavelet transforms in reversible data hiding using threshold based histogram modification. Journal of King Saud University – Computer and Information Sciences (2018), https://doi.org/10.1016/j.jksuci.2018.06.001

Table 5
Performance comparison with respect to PSNR and bit rate.

Method	Lena		Baboon		Airplane		Boat		Average	
	Bit rate (bpp)	PSNR (dB)	Bit rate (bpp)	PSNR (dB)	Bit rate (bpp)	PSNR (dB)	Bit rate (bpp)	PSNR (dB)	Bit rate (bpp)	PSNR (dB)
Ni et al. (2006)	0.020	48.20	0.020	48.20	0.228	48.70	0.027	48.20	0.074	48.325
Tai et al. (2009)	0.085	48.32	0.037	48.21	0.173	48.53	0.097	48.35	0.098	48.353
Chan et al. (2009)	0.152	44.78	0.039	39.09	0.167	44.61	0.003	45.51	0.09	43.498
Wu (2011)	0.161	44.25	0.056	44.27	-	-	0.129	44.23	0.115	44.25
Jinna and Ganesan (2010)	0.150	45.99	-	-	0.400	42.35	-	-	0.275	44.17
Yang (2007)	0.127	49.77	0.047	51.28	0.298	44.98	0.137	49.75	0.152	48.945
Haar	0.153	48.39	0.050	48.21	0.218	48.53	0.106	48.33	0.132	48.365
5/3	0.183	48.22	0.064	48.13	0.239	48.09	0.126	48.23	0.153	48.168
2/6	0.171	48.25	0.056	48.03	0.235	48.35	0.118	48.21	0.145	48.21
9/7	0.191	45.24	0.067	45.45	0.258	45.34	0.136	45.25	0.163	45.32
2/10	0.173	48.20	0.057	47.98	0.238	48.30	0.121	48.18	0.147	48.165
5/11-C	0.184	48.04	0.065	47.95	0.243	47.96	0.130	48.08	0.156	48.008
5/11-A	0.185	48.17	0.066	48.04	0.243	48.06	0.129	48.16	0.156	48.108
6/14	0.176	48.13	0.059	47.96	0.234	48.20	0.126	48.09	0.149	48.095
13/7-T	0.174	47.50	0.059	47.38	0.246	47.43	0.107	47.55	0.147	47.465
13/7-C	0.188	47.94	0.065	47.84	0.259	47.84	0.134	47.94	0.162	47.89
9/7-F	0.191	45.25	0.067	45.46	0.258	45.35	0.137	45.26	0.163	45.33

Table 6
Performance comparison between DWT (9/7) and integer wavelets (9/7-F, 9/7-M).

Image	Haung and Chang (2011)		9/7-F		9/7-M	
	PSNR (dB)	Bit rate (bpp)	PSNR (dB)	Bit rate (bpp)	PSNR (dB)	Bit rate (bpp)
Boat	31.41	0.149	45.24	0.136	48.01	0.131
Airplane	27.84	0.150	45.34	0.258	47.89	0.257
Lena	33.08	0.152	45.24	0.191	48.01	0.187

Table 7
Performance with respect to SSIM and bit rate.

Method/Transform	Lena		Baboon		Airplane		Boat		Average	
	Bit rate (bpp)	SSIM	Bit rate (bpp)	SSIM	Bit rate (bpp)	SSIM	Bit rate (bpp)	SSIM	Bit rate (bpp)	SSIM
Arsalan et al. (2012)	0.200	0.9920	0.100	0.9983	–	–	–	–	0.15	0.9952
Lin (2012)	0.236	0.9801	0.094	0.9929	0.484	0.9734	0.297	0.9751	0.2778	0.9804
Haar	0.386	0.9985	0.148	0.9993	0.468	0.9984	0.202	0.9992	0.301	0.9989
5/3	0.460	0.9953	0.127	0.9984	0.535	0.9952	0.241	0.9970	0.3408	0.9965
2/6	0.482	0.9985	0.111	0.9997	0.501	0.9984	0.226	0.9993	0.33	0.999
9/7-M	0.464	0.9949	0.127	0.9983	0.441	0.9962	0.247	0.9974	0.3198	0.9967
2/10	0.433	0.9989	0.112	0.9997	0.505	0.9984	0.229	0.9993	0.3198	0.9991
5/11-C	0.463	0.9951	0.129	0.9983	0.542	0.9952	0.246	0.9975	0.345	0.9965
5/11-A	0.464	0.9952	0.129	0.9984	0.542	0.9952	0.245	0.9975	0.345	0.9966
6/14	0.439	0.9979	0.115	0.9994	0.506	0.9978	0.238	0.9988	0.3245	0.9985
13/7-T	0.441	0.9918	0.117	0.9997	0.425	0.9948	0.208	0.9953	0.2978	0.9954
13/7-C	0.465	0.9955	0.128	0.9984	0.441	0.9965	0.253	0.9975	0.3218	0.997
9/7-F	0.477	0.9922	0.132	0.9975	0.440	0.9936	0.258	0.9954	0.3268	0.9947

Table 8
Difference in the histogram distribution.

Image	Haar	5/3	2/6	9/7-M	2/10	5/11-C	5/11-A	6/14	13/7-T	13/7-C	9/7-F
Elaine	0.0063	0.0061	0.0063	0.0062	0.0063	0.0063	0.0062	0.0063	0.0063	0.0062	0.0062
Baboon	0.0082	0.0077	0.0076	0.0075	0.0074	0.0075	0.0076	0.0072	0.0072	0.0074	0.0075
Fruits	0.0055	0.0053	0.0053	0.0053	0.0052	0.0053	0.0052	0.0054	0.0058	0.0052	0.0053
Home	0.0418	0.0444	0.0433	0.0445	0.0431	0.0455	0.0449	0.0443	0.0499	0.0448	0.0445
House	0.0117	0.0124	0.0118	0.0124	0.0118	0.0126	0.0126	0.0119	0.0143	0.0130	0.0124
Tiffany	0.0108	0.0101	0.0104	0.0099	0.0103	0.0099	0.0100	0.0101	0.0103	0.0100	0.0099
Lena	0.0069	0.0062	0.0062	0.0061	0.0061	0.0062	0.0062	0.0059	0.0068	0.0062	0.0061
Plane	0.0095	0.0084	0.0084	0.0079	0.0081	0.0080	0.0083	0.0080	0.0086	0.0080	0.0079
Boat	0.0169	0.0167	0.0166	0.0167	0.0165	0.0165	0.0166	0.0164	0.0169	0.0166	0.0167
Tanker	0.1353	0.1346	0.1346	0.1345	0.1345	0.1345	0.1346	0.1344	0.1346	0.1345	0.1345
Tree	0.0204	0.0197	0.0188	0.0190	0.0187	0.0191	0.0192	0.0190	0.0208	0.0190	0.0190
Average	0.0248	0.0247	0.0245	0.0245	0.0244	0.0247	0.0247	0.0244	0.0256	0.0246	0.0245

Please cite this article in press as: Shaik, A., Thanikaiselvan, V. Comparative analysis of integer wavelet transforms in reversible data hiding using threshold based histogram modification. Journal of King Saud University – Computer and Information Sciences (2018), https://doi.org/10.1016/j.jksuci.2018.06.001

Table 9
Performance with respect to auxiliary data.

Image	Wavelet	PSNR (dB)	Net data bits	Extra bits	Image	PSNR (dB)	Net data bits	Extra bits
Airplane					Lena			
	Chang et al. (2010)	43.71	74,656	54,416		43.43	62,784	68,288
	Tai et al. (2009)	48.53	45,472	20		48.32	22,377	20
	Liu et al. (2015)	45.26	74,332	4,568		44.77	50,077	4,240
	Haar	43.22	122,748	0		45.19	74,015	0
	5/3	44.56	111,732	0		44.49	88,999	0
	2/6	45.57	104,583	0		45.21	83,354	0
	9/7-M	44.52	115,793	0		44.46	90,259	0
	2/10	43.31	132,434	0		45.21	83,996	0
	5/11-C	44.43	113,123	0		44.36	89,636	0
	5/11-A	44.51	113,259	0		44.44	89,758	0
	6/14	43.22	132,733	0		45.03	85,193	0
	13/7-T	43.92	111,612	0		43.68	84,590	0
	13/7-C	44.58	115,859	0		44.48	90,758	0
	9/7-F	42.60	115,413	0		42.31	92,798	0
Baboon					Boat			
	Chang et al. (2010)	43.43	12,568	118,504		43.22	48,888	82,184
	Tai et al. (2009)	48.21	9,818	120		48.35	25,412	20
	Liu et al. (2015)	48.63	9,317	1,816		44.58	60,385	3,968
	Haar	44.51	26,297	74		42.05	74,905	50
	5/3	43.69	33,491	136		44.20	63,225	39
	2/6	44.48	29,204	72		44.90	59,428	0
	9/7-M	43.68	33,441	128		44.15	64,926	34
	2/10	44.47	29,516	76		44.92	60,196	25
	5/11-C	43.59	33,820	132		44.09	64,561	34
	5/11-A	43.63	33,943	134		44.13	64,301	30
	6/14	44.28	30,204	113		44.74	62,476	22
	13/7-T	42.89	30,780	143		43.39	54,541	29
	13/7-C	43.65	33,687	129		44.14	66,495	41
	9/7-F	42.04	34,807	160		42.19	67,892	49

Table 9 gives a comparison with respect to auxiliary data, embedding capacity and image quality. Here the term "net data bits" refers to the secret data hidden in the stego image and the term "extra bits" refers to the auxiliary data. From Table 9 it can be noted that as compared to (Chang et al., 2010; Tai et al., 2009; Liu et al., 2015) all the transforms required very small number of secret bits as auxilary data. As compared to the discrete haar wavelet transform based data hiding (Chang et al., 2010), the proposed integer transforms require very less amount of auxiliary data. Hence from the Table 9 a conclusion can be made that, the proposed data hiding technique achieves perfect restoration of the cover image with very small auxiliary data compared to state of art RDH techniques.

From the results, we have observed that, the stego image overflow and underflow pixels depends on the scaling factors of the integer wavelet transforms. The transforms with higher scaling factors like 3/7-T and 9/7-F generated the more out bounded pixels are compared with the lower scaling factor transforms like Haar, 5/3, 2/6 and 2/10. From all the results, it is obvious that a single transform cannot perform efficiently for all the images with all threshold combinations. The proposed methodology infers, that based on the user's need, proper integer transform must be chosen.

5. Conclusions

A threshold-based histogram shifting method has been successfully implemented in transform domain RDH. Several effective reversible integer transforms like 5/3, 2/6, 9/7-M, 2/10, 5/11-C, 5/11-A, 6/14, 13/7-T, 13/7-C and 9/7-F wavelet transforms employed for image coding and were duly adopted for the proposed RDH technique. Flag array technique has been employed as an overflow compensation mechanism. The performance of the integer wavelet transforms is compared with both spatial as well as transforms domain state of the art RDH methods. Exclusively, the performance with conventional DWT based methods and its counterpart integer wavelet versions are compared. It leads to the conclusion that the smaller scaling factor transforms like Haar, 2/6, 2/10 give higher PSNR at lower bit rates and the higher scaling factor transforms like 13/7-T and 9/7-F give lower PSNR images, and the transforms like 5/3, 9/7-M, 5/11-C, 5/11-A and 13/7-C give a medium performance. But for higher embedding rates, the transforms like 13/7-C, 6/14, 9/7-M, 5/11-C and 9/7-F perform better than Haar, 13/7-T and 5/3. As an inference, among all the eleven transforms, 2/6 and 2/10 provide consistent results. But clearly, no single transform can perform the best for all of the images. To suit individual user requirement specific wavelet transform must be chosen. One can see that this analysis leads to a better understanding of the relationship between the embedding capacity and the stego image quality whenever different wavelets were utilized.

References

Shi, Y., Li, X., Zhang, X., Wu, H.-T., Ma, B., 2016. Reversible Data Hiding: Advances in the Past Two Decades. IEEE Access 4, 3210–3237.

Bibi, N., Farwa, S., Muhammad, N., Jahngir, A., Usman, M., 2018. A novel encryption scheme for high-contrast image data in the Fresnelet domain. PLoS One 13 (4), 1–15.

Thanikaiselvan, V., Shastri, S., Ahmad, S., 2017. Information Hiding: Steganography. In: Intelligent Techniques in Signal Processing for Multimedia Security, vol. 660, pp. 65–91.

Shaik, A., Thanikaiselvan, V., Amitharajan, R., 2017. Data security through data hiding in images: a review. J. Artif. Intell. 10 (1).

Muhammad, N., Bibi, N., Qasim, I., Jahangir, A., Mahmood, Z., 2017. Digital watermarking using Hall property image decomposition method. Pattern Anal. Appl.

Tsai, P., 2009. Histogram-based reversible data hiding for vector quantisation-compressed images. Image Process. IET 3 (2), 100–114.

Qin, C., Chang, C.-C.C., Chen, Y.-C.C., 2013. Efficient reversible data hiding for VQ-compressed images based on index mapping mechanism. Signal Process. 93 (9), 2687–2695.

Lin, C.-C., Liu, X.-L., 2012. A Reversible Data Hiding Scheme for Block Truncation Compressions Based on Histogram Modification. 2012 Sixth Int Conf. Genet. Evol. Comput. 1, 157–160.

Fridrich, J., Goljan, M., Du, R., Aug. 2001. Invertible authentication. Secur. Watermarking Multimed. Contents 3, 197–208.

Please cite this article in press as: Shaik, A., Thanikaiselvan, V. Comparative analysis of integer wavelet transforms in reversible data hiding using threshold based histogram modification. Journal of King Saud University – Computer and Information Sciences (2018), https://doi.org/10.1016/j.jksuci.2018.06.001

Muhammad, N., Bibi, N., Mahmood, Z., Kim, D.G., 2015. Blind data hiding technique using the Fresnelet transform. Springerplus 4 (1), 1–15.
Nikolaidis, A., 2015. Reversible data hiding in JPEG images utilising zero quantised coefficients. IET Image Process. 9 (7), 560–568.
Lin, Y.-K., 2012. High capacity reversible data hiding scheme based upon discrete cosine transformation. J. Syst. Softw. 85 (10), 2395–2404.
Chan, Y.K., Chen, W.T., Yu, S.S., Ho, Y.A., Tsai, C.S., Chu, Y.P., 2009. A HDWT-based reversible data hiding method. J. Syst. Softw. 82 (3), 411–421.
Huang, H.-Y., Chang, S.-H., A 9/7 wavelet-based lossless data hiding. In: 2011 IEEE Symp. Comput. Intell. Multimedia, Signal Vis. Process., pp. 1–6, 2011.
Chang, C.C., Pai, P.Y., Yeh, C.M., Chan, Y.K., 2010. A high payload frequency-based reversible image hiding method. Inf. Sci. (Ny) 180 (11), 2286–2298.
Li, F., Mao, Q., Chang, C.-C., 2017. Reversible data hiding scheme based on the Haar discrete wavelet transform and interleaving prediction method. Multimed Tools Appl., 516
Agrawal, S., Kumar, M., 2016. Reversible data hiding for medical images using integer-to-integer wavelet transform. 2016 IEEE Students' Conf Electr. Electron. Comput. Sci., 1–5
Ni, Z.N.Z., Shi, Y.-Q.S.Y.-Q., Ansari, N., Su, W.S.W., 2006. Reversible data hiding. IEEE Trans. Circuits Syst. Video Technol. 16 (3), 354–362.
Tian, J., 2003. Reversible Data Embedding Using a Difference Expansion. IEEE Trans. Circuits Syst. 13 (8), 890–896.
Tai, W.-L., Yeh, C.-M., Chang, C.-C., 2009. Reversible Data Hiding Based on Histogram Modification of Pixel Differences. IEEE Trans. Circuits Syst. Video Technol. 19 (6), 906–910.
Liu, L., Chang, C.-C., Wang, A., 2015. Reversible data hiding scheme based on histogram shifting of n-bit planes. Multimed. Tools Appl. 66, 2015.
Wu, X., Zheng, X., 2011. Reversible Data Hiding Based on Histogram Shifting Using Difference Integer Wavelet Coefficients. 2011 Int Conf. Bus. Comput. Glob. Informatiz., 383–386
Jinna, S.K., Ganesan, L., 2010. Reversible image data hiding using lifting wavelet transform and histogram shifting. Int. J. Comput. Sci. Inf. Secur. 7 (3), 283–289.
Yang, L., Hao, P., Zhang, C., 2007. Progressive reversible data hiding by symmetrical histogram expansion with piecewise-linear haar transform. IEEE ICASSP, 265–268.
Arsalan, M., Malik, S.A., Khan, A., 2012. Intelligent reversible watermarking in integer wavelet domain for medical images. J. Syst. Softw. 85 (4), 883–894.
Muhammad, N. et al., 2017. Image de-noising with subband replacement and fusion process using bayes estimators. Comput. Electr. Eng.
Lee, S.K., Suh, Y.H., Ho, Y.S., 2006. Reversible image authentication based on watermarking. In: 2006 IEEE International Conference on Multimedia and Expo, ICME 2006 - Proceedings, 2006, vol. 2006, pp. 1321–1324.
Calderbank, A.R., Daubechies, I., Sweldens, W., Yeo, B.-L., 1998. Wavelet transforms that map integers to integers. Appl. Comput. Harmon. Anal. 5 (3), 332–369.
Le Gall, D., Tabatabai, A., 1988. Sub-band coding of digital images using symmetric short kernel filters and arithmetic coding techniques. Acoustics Speech Signal.
Villasenor, J.D., Belzer, B., Liao, J., 1995. Wavelet Filter Evaluation for Image Compression. IEEE Trans. Image Process. 4 (8), 1053–1060.
Strang, G., Nguyen, T., 1996. Wavelets and filter banks. Wellesley-Cambridge Press.
M. J. Gormish, E. L. Schwartz, A. F. Keith, M. P. Boliek, and A. Zandi, "Lossless and nearly lossless compression for high-quality images," in Proc. SPIE 3025, Very High Resolution and Quality Imaging, 1997, pp. 62–70.
Adams, M.D., Kossentini, F., 2001. Low-Complexity Reversible Integer-to-Integer Wavelet Transforms for Image Coding. In: 1999 IEEE Pacific Rim Conference on Communications, Computers and Signal Processing (PACRIM 1999). Conference Proceedings (Cat. No.99CH36368), 2001, pp. 1–4.
Adams, M.D., Kossentini, F., 2000. Reversible integer-to-integer wavelet transforms for image compression: performance evaluation and analysis. IEEE Trans. Image Process. 9 (6), 1010–1024.
Muhammad, N., Bibi, N., Mahmood, Z., Akram, T., Naqvi, S.R., 2017. Reversible integer wavelet transform for blind image hiding method. PLoS One 12 (5), 1–17.
Muhammad, N., Bibi, N., 2015. Digital image watermarking using partial pivoting lower and upper triangular decomposition into the wavelet domain. IET Image Process. 9 (9), 795–803.
Sweldens, W., 1995. The lifting scheme: A New Philosophy in Biorthogonal Wavelet Constructions. SPIE's 1995 Int Symp. Opt. Sci. Eng. Instrum. 2569, 68–79.
Ma, B., Shi, Y.Q., 2016. A Reversible Data Hiding Scheme Based on Code Division Multiplexing. IEEE Trans. Inf. Forensics Secur. 11 (9), 1914–1927.
Zhang, T., Ping, X., Oct. 2003. A new approach to reliable detection of LSB steganography in natural images. Signal Process. 83 (10), 2085–2093.

Ahmad Shaik is a research associate at VIT University Vellore, India. He received his BTech and MTech degrees in Electronics and Communication Engineering and Digital Electronics and Communication Systems from the JNTU University, Anantapur in 2012 and 2015, respectively. And he is currently pursuing PhD in VIT University Vellore, India. He is the author of two journal papers and has written a book chapter. His current research interests include reversible data hiding and integer wavelet transforms.

DR. Thanikaiselvan V received his Ph.D. degree in the field of Information security form VIT university, Vellore, Tamilnadu in the year 2014. He received MTech in Advanced Communication Systems from SASTRA University, Thanjavur, in 2006 and B.E in Electronics and Communication Engineering form Bharathidasan University, Trichy, in 2002. He joined VIT University in 2006 as a Lecturer and Currently working as an Associate Professor in Department of Communication Engineering under the School of Electronics Engineering, VIT University, Vellore. His teaching and research interest includes Digital communication, Wireless communication, Digital signal and Image Processing, Wireless Sensor Networks and Information Security. He has published more than 30 research articles. Currently he is guiding 4 Ph.D. candidates in the areas of Information Security and Digital Image Processing. He is an active IEEE member and reviewer for Elsevier, Wiley and springer journals.

Please cite this article in press as: Shaik, A., Thanikaiselvan, V. Comparative analysis of integer wavelet transforms in reversible data hiding using threshold based histogram modification. Journal of King Saud University – Computer and Information Sciences (2018), https://doi.org/10.1016/j.jksuci.2018.06.001